

See discussions, stats, and author profiles for this publication at: <https://www.researchgate.net/publication/231652106>

# Interaction of the Photosensitizer Hypericin with Low-Density Lipoproteins and Phosphatidylcholine: A Surface-Enhanced Raman Scattering and Surface-Enhanced Fluorescence Study

ARTICLE in THE JOURNAL OF PHYSICAL CHEMISTRY C · APRIL 2009

Impact Factor: 4.77 · DOI: 10.1021/jp8112528

CITATIONS

11

READS

40

5 AUTHORS, INCLUDING:



**Daniel Jancura**

Pavol Jozef Šafárik University in Košice

43 PUBLICATIONS 488 CITATIONS

SEE PROFILE



**José Vicente García-Ramos**

Spanish National Research Council

177 PUBLICATIONS 3,796 CITATIONS

SEE PROFILE



**S. Sanchez-Cortes**

Spanish National Research Council

197 PUBLICATIONS 4,204 CITATIONS

SEE PROFILE

# Interaction of the Photosensitizer Hypericin with Low-Density Lipoproteins and Phosphatidylcholine: A Surface-Enhanced Raman Scattering and Surface-Enhanced Fluorescence Study

G. Lajos,<sup>†</sup> D. Jancura,<sup>†</sup> P. Miskovsky,<sup>†,§</sup> J. V. García-Ramos,<sup>‡</sup> and S. Sanchez-Cortes<sup>\*,‡</sup>

Department of Biophysics, Safarik University, Jesenna 5, 041 54 Kosice, Slovakia, Instituto de Estructura de la Materia, CSIC, Serrano 121, 28006 Madrid, Spain, and International Laser Centre, Ilkovicova 3, 812 19 Bratislava, Slovakia

Received: December 19, 2008; Revised Manuscript Received: March 4, 2009

Surface-enhanced Raman spectroscopy (SERS) and surface-enhanced fluorescence were utilized for the study of the interaction of the photosensitizer hypericin (Hyp) with low-density lipoproteins (LDL) and phosphatidylcholine (PCH). The obtained results provided data for the construction of a simple model of Hyp/LDL complex at different Hyp/LDL concentration ratios. We have proposed in this model that at low Hyp/LDL ratios (<50:1) molecules of Hyp, which exist under these conditions in a monomeric state, are localized between the hydrophobic core and outer shell of the LDL, and when the concentration of Hyp increases, these molecules are mostly placed in the outer phospholipid shell where the aggregates of Hyp are formed. This model is mainly based on the observation that the fluorescence of monomeric Hyp in the complex of LDL is substantially quenched in the presence of silver nanoparticles. In contrast, the intensity of emission of the Hyp excimer is relatively enhanced at high Hyp/LDL values (>50:1). Moreover, the SERS spectra of the Hyp/LDL complex at high Hyp/LDL ratios demonstrate the predominance of monoanionic form of Hyp, which confirms that at these high ratios the molecules of Hyp are localized in the outer shell of the LDL molecule.

## Introduction

Hypericin (Hyp), 1,3,4,6,8,13-hexahydroxy-10,11-dimethylphenanthro[1,10,9,8-*opqra*]perylene-7,14-dione (Figure 1), is a naturally photosensitizing pigment occurring in plants of the genus *Hypericum* and some insect species. The recent interest in Hyp is due to the discovery that under light illumination Hyp possesses antiproliferative and cytotoxic effects (necrosis as well as apoptosis) on many tumor cell lines and virucidal activity against several types of enveloped viruses. These properties together with minimal dark toxicity, its tumor selectivity, and the high clearance rate from the host body make Hyp a very promising agent for photodynamic therapy (PDT) of cancer and virus diseases.<sup>1–3</sup>

It is well-known that serum proteins are predominantly responsible for the transportation of photosensitizers throughout the body.<sup>4–9</sup> Upon administration into the bloodstream Hyp associates mainly with low-density lipoproteins (LDL) and to a lesser extent with human serum albumin (HSA) and high-density lipoproteins (HDL).<sup>10</sup>

LDL could play a key role in the targeted delivery of hydrophobic and/or amphiphilic photosensitizers to tumor cells in PDT,<sup>5–9,11–15</sup> due to the enhanced expression of specific LDL receptors (regulated by the cholesterol needs of the cell, usually higher in fast growing cells, like tumor cells and tumor endothelial cells) in many types of transformed cells when compared with nontransformed cells.<sup>12,16,17</sup> LDL particles have a spherical shape and a size of ca. 22 nm, with a hydrophobic lipidic core consisting of above 170 triglyceride and 1600 cholesteryl ester molecules and the amphipathic outer shell

comprising about 700 phospholipid molecules and a single copy of apolipoprotein B-100 (apoB-100) (Figure 1b).<sup>18</sup> In addition, the particles contain about 600 molecules of unesterified cholesterol, of which about one-third is located in the core and two-thirds in the surface of LDL.

Our previous studies in the field of Hyp/LDL interactions by steady-state and time-resolved fluorescence and phosphorescence spectroscopy showed that high Hyp/LDL ratios (>30:1) lead to a significant decrease of quantum yield and lifetime of Hyp fluorescence.<sup>19–21</sup> We have suggested that this decrease is caused by the formation of nonfluorescent Hyp aggregates inside of LDL molecules as well as by the self-quenching of Hyp fluorescence.<sup>19</sup> On the other hand, the kinetics of the depopulation of the triplet excited state of Hyp is not significantly dependent on Hyp concentration. It was also proposed that the primary process of depopulation of Hyp triplet state inside LDL is its interaction with ground-state molecular oxygen with consequent production of singlet oxygen.<sup>20</sup> It was shown that photoactivated Hyp oxidizes LDL in a light dose and excitation wavelength dependent manner. We have also demonstrated an important role of the LDL receptor pathway for Hyp delivery to U-87 MG cells in the presence of LDL.<sup>22</sup> The substantial increase of Hyp uptake was revealed in the situation when the number of LDL receptors on the cell surface was elevated. Moreover, the colocalization experiments showed the lysosomal localization of Hyp following the uptake and that the concentration of Hyp in these organelles was enhanced in the cells with an elevated number of LDL receptors when incubation medium contained LDL.<sup>22</sup>

Raman spectroscopy could afford important information about the mechanism of the aggregation undergone by Hyp in aqueous solutions or when interacting with biological molecules. How-

<sup>†</sup> Safarik University.

<sup>§</sup> International Laser Centre.

<sup>‡</sup> Instituto de Estructura de la Materia, CSIC.

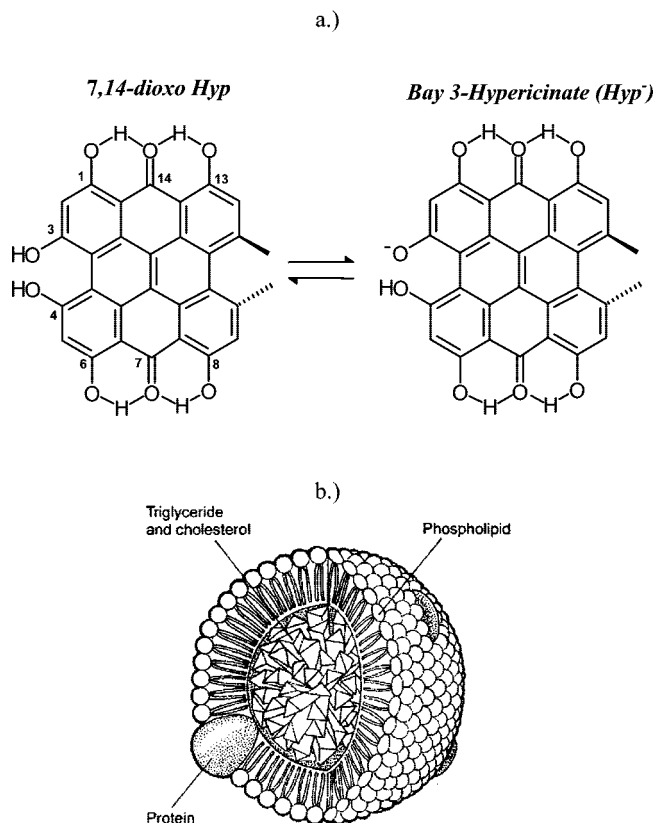


**Figure 1.** Molecular structure of neutral and monoanionic hypericin (a) and model of LDL molecule (b).

ever, the application of this technique is highly limited by the large fluorescence emission of Hyp. These drawbacks can be overcome when using metal nanoparticles (NPs) to partially quench the fluorescence emission and to enhance the Raman spectrum by surface-enhanced Raman scattering (SERS). NPs irradiated with a visible light of appropriate wavelength can induce a great intensification of the electromagnetic field on the surface through localized surface plasmon resonance which consequently leads to a great enhancement of Raman signal from molecules adsorbed on NPs.<sup>23,24</sup> These phenomena then allowed the Raman study of Hyp and its interaction with biomolecules on silver NPs (AgNPs).<sup>25–29</sup>

Although the fluorescence is quenched on the surface of AgNPs, at a proper distance from the surface (more than 50 Å) the emission of a fluorophore can be enhanced leading to a surface-enhanced fluorescence (SEF) effect, which is particularly strong at distances between 70 and 100 Å.<sup>30</sup> At these conditions a combined SERS+SEF emission spectrum can be obtained, thus providing a joint vibrational and electronic information about molecules adsorbed on metal NPs.<sup>31,32</sup> In order to place the fluorophore at a proper distance from the metal, the surface of this metal must be functionalized with a spacer. This was accomplished by covering the NPs with spacers such as fatty acids,<sup>31,32</sup> or proteins.<sup>33</sup> LDL can also play the role of a spacer, since the diameter of this lipoprotein is about 220 Å.<sup>18</sup> Thus, the emission spectra of Hyp/LDL complexes are expected to possess fluorescence and Raman signals from both the lipoprotein and Hyp containing rich information about many interesting processes occurring in this biological complex: drug–carrier interaction, Hyp aggregation, and its distribution inside the LDL particles.

The aim of this work is to apply both SERS and SEF to obtain comprehensive information about vibrational and fluorescent

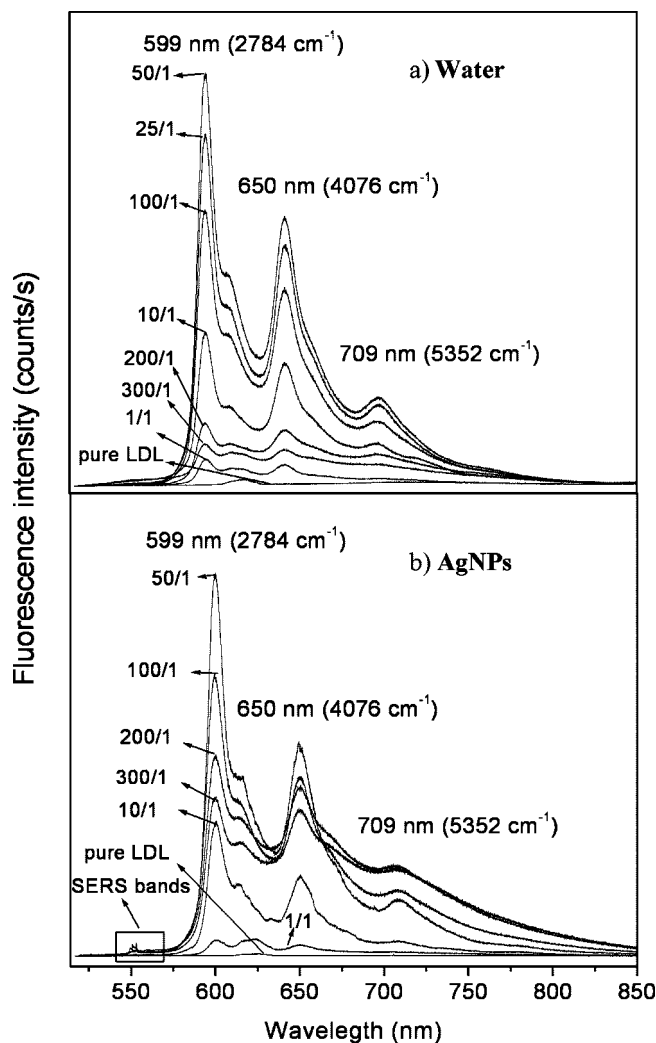


**Figure 2.** Fluorescence and Raman spectra of Hyp/LDL complexes at different concentration ratios in water (a) and on AgNPs (b). The concentration of LDL was maintained constant at  $10^{-8}$  M. Excitation line 514.5 nm.

properties of Hyp molecules incorporated into LDL and contribute to the more detailed characterization of the localization of Hyp inside LDL at different Hyp/LDL ratios. Moreover, the interaction of Hyp with phosphatidylcholine (PCH) as one of the main components of the outer shell of LDL is investigated as well.

## Experimental Section

**Preparation of Silver Nanoparticles.** Silver nanoparticles (AgNPs) were prepared by chemical reduction of silver nitrate with hydroxylamine hydrochloride.<sup>34</sup> The resulting colloid showed a milky gray color with a final pH of 5.5. The aqueous solutions utilized for the AgNPs formation were prepared by using triply distilled water, and all the reagents employed were purchased from Sigma.

**Preparation of Hyp/LDL Solutions and Samples for SERS+SEF Experiments.** The stock solution of Hyp (Sigma) ( $c = 1.92 \times 10^{-3}$  M) was prepared by dissolving the drug in 100% dimethyl sulfoxide (DMSO) and was kept in the dark at 4 °C. LDL was purchased as an aqueous solution (Calbiochem-VWR, France) at a concentration of  $1.28 \times 10^{-5}$  M containing NaCl (150 mM) and 0.01% ethylenediaminetetraacetic acid (EDTA). The pH of this solution was 7.4. Solutions of Hyp/

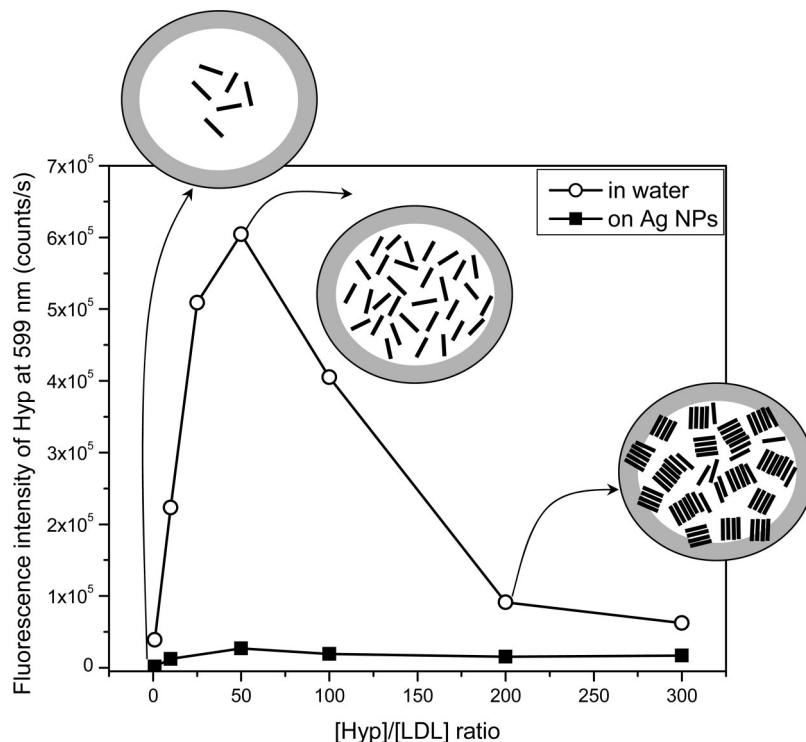


**Figure 3.** Dependence of the fluorescence intensity (maximum at 599 nm) of Hyp on Hyp/LDL ratio in water (O) and in the presence of Ag NPs (■). Inset: Model of localization and aggregation state of Hyp inside LDL at different Hyp/LDL ratios.

LDL complexes were prepared by dilution and mixing of stock solutions of LDL and Hyp in milli-Q water. The experiments were carried out while maintaining constant the concentration of LDL at  $10^{-8}$  M and varying the concentrations of Hyp between  $10^{-8}$  and  $3 \times 10^{-6}$  M. The final quantity of DMSO in all solutions used in the experiments was less than 1%. The solutions of Hyp/LDL complexes were added to milli-Q water or the activated colloidal suspension of AgNPs and then stored in the dark for 2 h before measurements. The activating of the colloid was made by aggregation of Ag NPs induced by adding of 30  $\mu$ L of 0.5 M  $\text{KNO}_3$  to 1 mL of the colloid. The final pH of the solutions of Hyp/LDL in water and silver colloids was 6.0.

**Preparation of Hyp/PCH Solution.** In this case the concentration of Hyp was kept at  $10^{-6}$  M, while the concentration of PCH was varied from  $10^{-8}$  to  $10^{-3}$  M. The aqueous solutions of PCH from soybean (Sigma, purity 99% (TLC)) were prepared at a concentration 1 order of magnitude higher than that required for the final desired one. Then 890  $\mu$ L of triply distilled water or activated colloidal solution (in the case of SEF and SERS measurements) was added to 100  $\mu$ L of the PCH solution. After 30 min, 10  $\mu$ L of the Hyp solution in DMSO ( $c = 10^{-5}$  M) was added to the final mixture.

**Instrumentation.** The SEF+SERS spectra of Hyp, LDL, and Hyp/LDL complexes were measured with a Renishaw micro-Raman system (RM2000) using as excitation the  $\text{Ar}^+$  laser line at 514.5 nm. This instrument was equipped with a Leica microscope and an electrically refrigerated CCD camera. The signal was calibrated by using the 520  $\text{cm}^{-1}$  line of a Si wafer and a 50 $\times$  objective. SEF+SERS measurements were realized using a macro-Raman configuration by using a macro device provided by Renishaw and a 30 mm lens. Samples in solution were placed in a 1  $\times$  1 cm glass cuvette. The laser power on the sample was 2 mW. The resolution was set to 4  $\text{cm}^{-1}$  and five scans of 10 s each were averaged. Spectra were recorded in the 200–8000  $\text{cm}^{-1}$  region to observe both the Raman and fluorescence spectra.

## Results and Discussion

**Hyp/LDL Complex.** The fluorescence and Raman spectra of Hyp/LDL complexes were studied in water and on AgNPs (parts a and b of Figure 2, respectively). The experiments were realized at different Hyp/LDL ratios maintaining the constant concentration of LDL at  $10^{-8}$  M. The fluorescence spectra of Hyp in the presence of LDL particles have already been studied in our previous works showing a significant decrease of quantum yield and lifetime of Hyp fluorescence at high Hyp/LDL ratios (>50:1).<sup>19–21</sup>

In water an increase of the intensity of the main fluorescence peak of Hyp (maximum at 599 nm) with the increase of Hyp concentration is observed in the range of the concentration ratios between 1:1 and 50:1 (Figure 3). The fluorescence spectra observed in this interval correspond to the Hyp monomer, as corroborates the similarity with the spectrum of Hyp in DMSO.<sup>19</sup> For higher Hyp/LDL ratios (>50:1), a significant decrease of this fluorescence is detected. This result indicates that Hyp interacts with LDL under the monomeric form up to a 50:1 ratio (Figure 3, inset scheme), and above this value Hyp molecules begin to aggregate upon accumulation inside the LDL structure (Figure 3, inset). The fluorescence quenching is attributed to the drug aggregation, which is responsible for the significant decrease of Hyp fluorescence observed at these high concentration ratios, but partially also to the dynamic self-quenching of the singlet excited state of Hyp.<sup>19,20</sup> No Raman bands of Hyp are observed in water due to the poor Raman emission in the absence of AgNPs.

A broad emission with an apparent center at 709 nm is observed when the Hyp/LDL ratio increases (Figure 2). This emission is better seen in the difference spectra (Figure 4a,b) and can be assigned to the excimer emission, which is provoked by the formation of H-aggregates of Hyp, as demonstrated in our previous work.<sup>29</sup> In Figure 4c the intensity of the excimer emission is plotted as a function of the Hyp/LDL ratio. As can be observed, the intensity of excimer emission increases for Hyp/

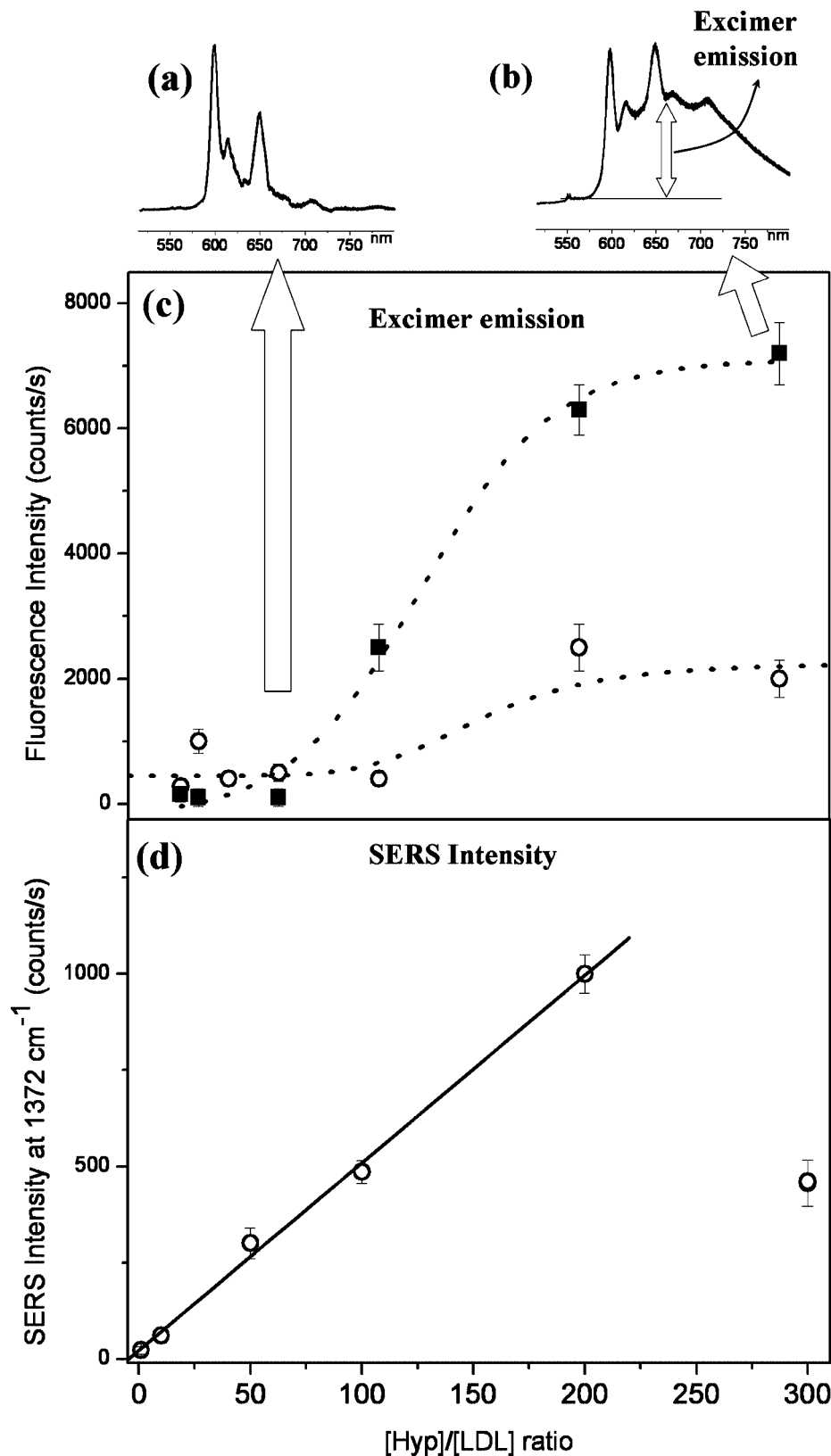


**Figure 4.** Difference emission spectra obtained by subtracting the spectrum of Hyp in DMSO from the fluorescence spectra at 50:1 (a) and 300:1 (b) Hyp/LDL ratios. (c) Plot of the excimer emission in the absence (○) and the presence (■) of AgNPs. (d) Variation of SERS intensity with the Hyp/LDL ratio measured for the band at 1372 cm<sup>-1</sup>.

LDL ratios above 50:1, just at the same ratio at which the corresponding monomer emission at 599 nm decreases.

The fluorescence emission of the Hyp/LDL complex undergoes a significant intensity decrease in the presence of AgNPs (Figure 3b). This is a consequence of fluorescence quenching

caused by the energy transfer between Hyp molecules localized inside LDL and metal colloid particles as well as by the absorption of part of the photons emitted from Hyp molecules by AgNPs. This phenomenon is usually observed when studying fluorescent molecules in the presence of metal nanoparticles.<sup>34</sup>



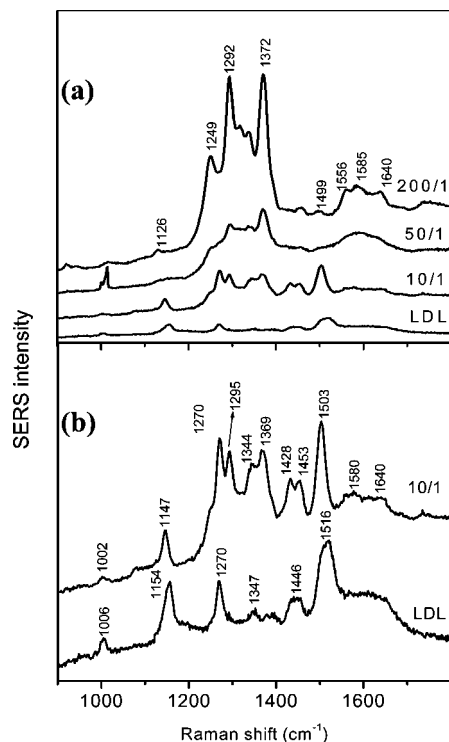


**Figure 5.** (a) SERS spectra of LDL and Hyp/LDL complexes at the following concentration ratios: 10:1, 50:1, 200:1. (b) Comparison between the SERS spectra of LDL alone ( $\times 3$ ) and the Hyp/LDL complex at 10:1 ratio. The concentration of LDL was  $10^{-8}$  M. The excitation line was 514.5 nm.

The quenching was not compensated by an intensification of the fluorescence by SEF effect due to the long distance between Hyp molecules and the metal surface. This result points out that at low Hyp concentrations the drug is rather placed in the interior part of LDL, where the distance to the metal surface is too far to undergo a SEF enhancement.

The fluorescence quenching of the monomer is opposite to the enhancement of the excimer emission associated to Hyp aggregates observed for high Hyp/LDL ratios on Ag NPs (Figure 4c). This enhancement is attributed to two different reasons: the increase of Hyp aggregates in the LDL particle and the closer position of these aggregates in relation to the metal surface, since they tend to be localized in the external part of the LDL particles as the concentration of Hyp is increased. Both effects are further amplified as the Hyp/LDL ratio is increased.

More detailed information about the host and the ligand structures can be obtained from the SERS spectra. The SERS spectra of Hyp/LDL at different ratios are shown in Figure 5a. The SERS spectrum of LDL alone is also amplified in Figure 5b. This spectrum displays strong features at 1006, 1154, and 1516  $\text{cm}^{-1}$ , which correspond to carotenoid compounds normally existing in LDL structure, in particular all-*trans*- $\beta$ -carotene and lycopene.<sup>35,36</sup> These bands are attributed to the in-phase C=C stretching vibrations in the central part of the chain, the C-C stretching also from bonds in the central part, and in-phase combinations of in-plane rocking motions contributed by the  $\text{CH}_3$  groups.<sup>37,38</sup> In addition, the bands at 1270, 1347, and 1430–60  $\text{cm}^{-1}$  could be attributed to the aliphatic chains of lipidic species existing in LDL.

The SERS spectrum of Hyp/LDL complex at the 10:1 ratio exhibited a mixture of bands due to both LDL and Hyp (Figure 5b). However, the SERS intensity of Hyp is weaker than the main bands of LDL due to the long distance of Hyp molecules

from the NPs, suggesting again that the drug is located in the inner part of the LDL particle at this low ratio. Moreover, a general intensification is observed for the bands of carotenoid compounds in the presence of Hyp, which also underwent a shift to lower wavenumbers (1006  $\rightarrow$  1002  $\text{cm}^{-1}$ , 1154  $\rightarrow$  1147  $\text{cm}^{-1}$ , and 1516  $\rightarrow$  1503  $\text{cm}^{-1}$ ). The enhancement of the Raman bands of carotenoids could be due to (a) the structural modification of the carotenoids inside the LDL in the presence of Hyp or (b) an energy transfer mechanism provoked by the large absorption and emission of light by Hyp, and which specifically favors the preresonance Raman effect of lycopene in particular. This is supported by the fact that lycopene has an absorption band at above 500 nm.<sup>35–37,39</sup>

The SERS intensity of Hyp, analyzed for the most intense band at 1372  $\text{cm}^{-1}$ , increases linearly with the increase of Hyp/LDL ratio (Figure 4d). Two different effects are contributing to this: (a) the increase of Hyp concentration and (b) the progressive localization of Hyp molecules in the outer shell of LDL, which is obviously closer to the metal surface than the hydrophobic core of LDL.

The analysis of the SERS spectra affords detailed structural information since the Raman spectra can be considered as molecular fingerprints showing a different structure of the molecules. At relatively low Hyp/LDL ratios ( $<50:1$ ) the SERS spectrum of Hyp corresponds to a mixture of neutral and monoanionic forms, which is deduced on the basis of the results of our previous work, where pH dependency of the SERS spectra of Hyp was studied.<sup>29</sup> At high Hyp/LDL ratios ( $\sim 200:1$ ) the contribution of the monoanionic form, characterized by the SERS bands at 1249, 1293, and 1372  $\text{cm}^{-1}$ , is dramatically increased. This indicates that at very high concentrations Hyp molecules are placed in a more polar environment, i.e., in the amphipathic outer part of the LDL particle as already proposed in our previous work.<sup>19,20</sup> Since in this region phospholipids and apoB-100 proteins are localized, an interaction of the hypericin with the polar groups of these biomolecules is likely occurring.

In Figure 6 a summary picture of the variation of the fluorescence of monomer Hyp, excimer emission, and SERS intensity of Hyp/LDL complex at different concentration ratios is shown. This scheme is based on the combination of the data coming out from the SERS band at 1372  $\text{cm}^{-1}$ , the fluorescence spectra of monomers (emission at 599 nm), and the excimer emission (apparent maximum at 709 nm). It is proposed that at low Hyp/LDL ratios ( $<50:1$ ) molecules of Hyp are dominantly localized in the region between the hydrophobic core and the phospholipid outer shell of LDL where Hyp molecules exist under monomeric form. Above this ratio the fluorescence of the monomer form and the excimer of Hyp aggregates undergo a different behavior. The sigmoidal dependence of the intensity of excimer emission against the Hyp/LDL ratio is probably due to the sum of many effects: Hyp aggregation, higher relative concentration of Hyp in outer shell of LDL in comparison with the core of LDL molecule at high Hyp/LDL ratios, and quenching of the emission of molecules whose distance to the surface is below 50 Å. In contrast, the SERS intensity of Hyp undergoes an almost linear growing until Hyp/LDL = 200/1 ratio. This is due to the fact that this intensity is practically unaffected by the drug aggregation. The interaction model for the Hyp/LDL complex depicted in Figure 3 fully correlates with our recent and previous data.<sup>19–21</sup>

**PCH/Hyp Complex.** In order to have more information about the possible interaction of Hyp with LDL in the outer region of the lipoprotein, we have investigated the interaction of Hyp with

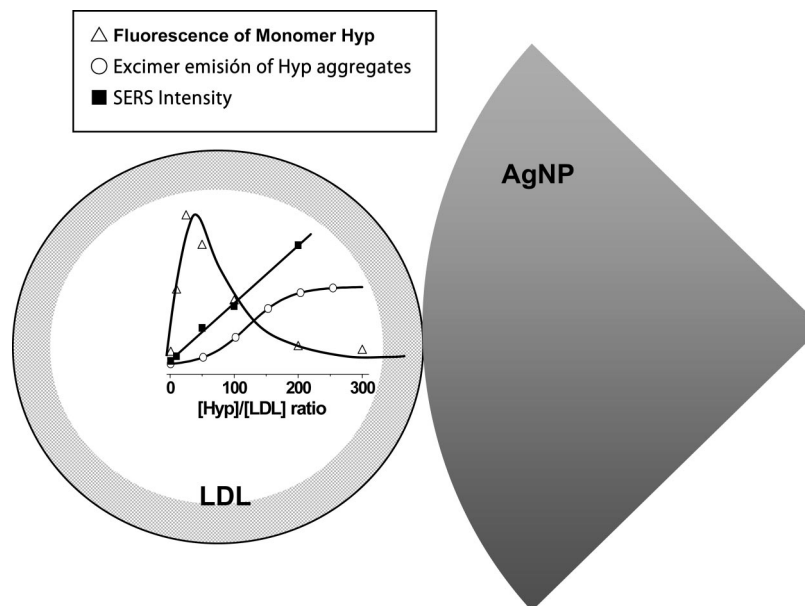


**Figure 6.** Fluorescence of the Hyp monomers (at 599 nm), the excimer emission of Hyp aggregates (at 709 nm), and the SERS intensity of 1372  $\text{cm}^{-1}$  band as functions of Hyp/DL ratio. These variations were correlated to the possible approach of the drug to the metal surface of AgNP.

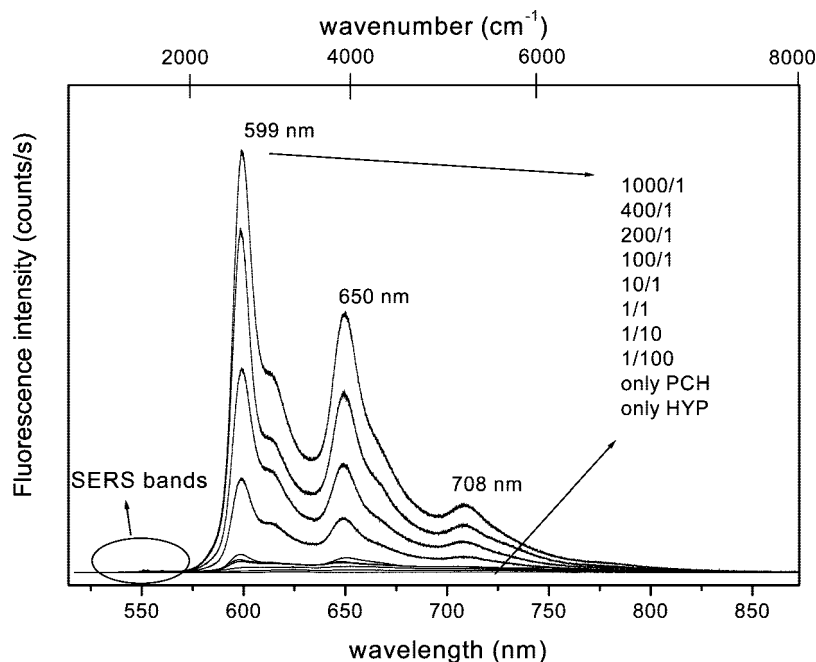


**Figure 7.** Fluorescence and Raman spectra of PCH/Hyp complexes at different concentration ratios on AgNPs. The concentration of Hyp was  $10^{-6}$  M. Excitation line 514.5 nm.

PCH, the main phospholipid component of the LDL surface monolayer.<sup>18</sup> The fluorescence and Raman spectra of the PCH/Hyp complexes were investigated both in water and on AgNPs (Figure 7). The experiments were realized at different PCH/Hyp ratios, maintaining constant the concentration of Hyp at  $10^{-6}$  M. The Hyp fluorescence intensity represented by the most intense band at 599 nm is plotted against the PCH/Hyp ratio in Figure 8 both in the absence and in the presence of AgNPs. It is observed that the fluorescence of Hyp increases with the increase of PCH/Hyp. This is attributed to the interaction of Hyp with PCH molecules and, consequently, to the formation of fluorescent monomers of Hyp. It is observed that for the fully monomerization of Hyp, several hundred ( $\sim 200$ – $300$ ) PCH molecules should be present for each Hyp molecule.

Contrary to the properties of the fluorescence of Hyp/LDL complex, the fluorescence intensity of Hyp in the presence of

PCH is not quenched by the AgNPs. In addition, a SEF of Hyp is observed at PCH/Hyp ratios above 200:1. These phenomena are probably due to a covering of the metal surface by PCH molecules, assuming that PCH molecules are directly linked to the surface of the particles as reported by several authors for other kinds of phospholipids,<sup>40,41</sup> which hinder the direct contact of Hyp to the metal. At a PCH/Hyp = 200:1 ratio, which corresponds to PCH concentration of  $2 \times 10^{-4}$  M, PCH molecules fully covered metal nanoparticles forming bilayers or multilayers. At these conditions, PCH molecules act as spacers and the Hyp monomers are dispersed in the PCH multilayers and placed far away from the surface (Figure 8, top right scheme). Such geometrical arrangement does not lead to the quenching of Hyp fluorescence but rather to its enhancement due to the SEF effect. This effect seems not to occur at low PCH concentrations (PCH/Hyp < 50:1) at which

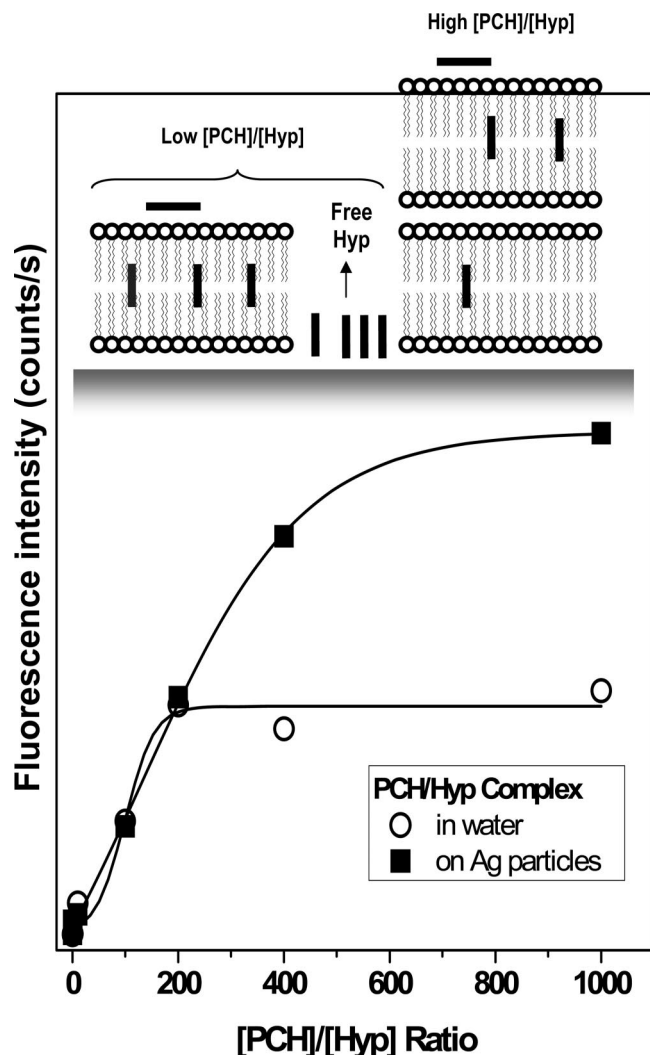


**Figure 8.** Dependence of the fluorescence intensity (maximum at 599 nm) of Hyp on PCH/Hyp ratio in water (○) and in the presence of AgNPs (■). Top: Schemes of the most probable position of Hyp molecules in PCH bilayers and multibilayers at low and high PCH/Hyp ratios.

the coverage of the metal surface by PCH is incomplete and a large amount of free molecules of Hyp (nonincorporated into PCH bilayers or multibilayers) exist in the system (Figure 8, top left scheme).

The SERS intensity of Hyp follows an opposite behavior in comparison with the fluorescence of a PCH/Hyp complex (Figure 9). At low values of PCH/Hyp ratio the SERS intensity is high due to both the direct interaction of free Hyp with metal surface or its close proximity to the surface when interacting with PCH bilayers (Figure 8, top left scheme). On the other hand at high PCH/Hyp ratios the SERS intensity is weakened due to the progressive covering of the metal surface by PCH which consequently leads to a more difficult approach of Hyp molecules to the metal surface.

At low ratios, the SERS spectrum is dominated by the monoanionic Hyp form (Figure 9, upper spectra), since intense bands are observed at 1240 and 1288  $\text{cm}^{-1}$ , mainly attributed to Hyp directly adsorbed onto the surface under the monoanionic form. However, at high PCH/Hyp ratios ( $>100:1$ ) the SERS profile (Figure 9, lower spectra) is more similar to the neutral form attributed to the monomeric Hyp inserted in the bilayers or multibilayers formed by PCH on the metal surface at these high ratios.

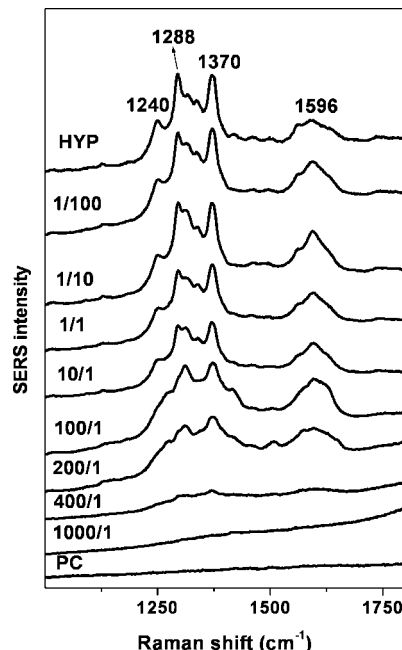


**Figure 9.** SERS spectra of Hyp alone, PCH/Hyp complexes at different concentration ratios, and PCH alone ( $10^{-6}$  M). The concentration of Hyp was  $10^{-6}$  M. The excitation line was 514.5 nm.

These results are in accordance with our previous work and suggestions<sup>19,20</sup> that the most probable region for the internalization of Hyp into LDL is the polar zone close to the phospholipid–water interface, but with the increase of Hyp/LDL ratio the population of Hyp molecules localized in a more hydrophobic part of LDL (e.g., region of fatty acid chains in phospholipids) is increased.

## Conclusions

SERS and SEF spectra of Hyp/LDL and PCH/Hyp complexes afforded key information about the distribution of Hyp in the supramolecular complexes of these biomolecules. Significant quenching of the fluorescence of Hyp molecules incorporated in LDL in the presence of AgNPs was observed; however the excimer emission is relatively enhanced to the emission of monomeric Hyp, mainly at high Hyp/LDL ratios ( $>50:1$ ). This is due to SEF effect on Hyp aggregates which tend to be localized in the outer shell of LDL molecules. SERS spectra of Hyp/LDL revealed that at low Hyp/LDL ratios the Raman spectrum of Hyp consists of a mixture of Raman spectra for neutral and monoanionic forms, on the other hand the increase of Hyp concentration leads to the SERS spectrum in which features of the SERS spectrum of monoanionic form dominate. This observation confirms that at high Hyp/LDL ratios molecules of Hyp are placed in the outer shell of LDL, where they form aggregates. The SEF and SERS data on Hyp/LDL provided a solid base for the construction of a simple model of the Hyp/LDL complex at different concentration ratios. In this model we have proposed that at low Hyp/LDL ratios ( $<50:1$ ) molecules of Hyp, which exist under these conditions in a monomeric state, are localized between hydrophobic core and outer shell of LDL, and when the concentration of Hyp increases, these molecules are mostly placed in the outer phospholipid shell where the aggregates of Hyp are formed.

Intensities of the fluorescence and SERS spectra of PCH/Hyp complexes behave in opposite directions. The increase of PCH/Hyp ratio leads to the enhancement of Hyp fluorescence



but to the considerable decrease of SERS intensity. This is caused by the fact that at high PCH concentrations the molecules of Hyp are localized in bilayers/multilayers of PCH which cover the surface of AgNPs remaining far away from the surface.

**Acknowledgment.** This work was supported by the Slovak Research and Development Agency under Contract APVV-0449-07, the Scientific Grant Agency of the Ministry of Education of Slovakia under Grant VEGA 4449/07, CSIC-Slovak Academy of Science Project No. 2007SK0002, the SPP Foundation (G.L.), the Ministerio de Educación y Ciencia of Spain Project No. FIS2007-63065, and the Comunidad de Madrid Project No. S-0505/TIC/0191 MICROSERES. This work forms a part of PhD thesis of G.L.

## References and Notes

- (1) Agostinis, P.; Vantieghem, A.; Merlevede, W.; de Witte, P. *Int. J. Biochem. Cell Biol.* **2002**, *34*, 221.
- (2) Falk, H. *Angew. Chem., Int. Ed.* **1999**, *38*, 3116.
- (3) Kiesslich, T.; Krammer, B.; Plaetzer, K. *Curr. Med. Chem.* **2006**, *13*, 2189.
- (4) Miskovsky, P. *Curr. Drug Targets* **2002**, *3*, 55.
- (5) Derycke, A. N. L.; de Witte, P. *Adv. Drug Delivery Rev.* **2004**, *56*, 17.
- (6) Jori, G. *J. Photochem. Photobiol., B* **1996**, *36*, 87.
- (7) Konan, Y. N.; Gurny, R.; Alleman, E. *J. Photochem. Photobiol., B* **2002**, *66*, 89.
- (8) Reddi, E. *J. Photochem. Photobiol., B* **1997**, *37*, 189.
- (9) Sherman, W. M.; van Lier, J. E.; Allen, C. M. *Adv. Drug Delivery Rev.* **2004**, *56*, 53.
- (10) Chen, B.; Xu, Y.; Roskams, T.; Delaey, E.; Agostinis, P.; Vandenheede, J. R.; de Witte, P. *Int. J. Cancer* **2001**, *93*, 275.
- (11) Polo, L.; Valduga, G.; Jori, G.; Reddi, E. *Int. J. Biochem. Cell Biol.* **2002**, *34*, 10.
- (12) Firestone, R. A. *Bioconjugate Chem.* **1994**, *5*, 105.
- (13) Jori, G.; Reddi, E. *Int. J. Biochem.* **1993**, *25*, 1369.
- (14) Maziere, J. C.; Moliere, P.; Santus, R. *J. Photochem. Photobiol., B* **1991**, *8*, 351.
- (15) Bonneau, S.; Vever-Bizet, C.; Morliere, P.; Maziere, J. C.; Brault, D. *Biophys. J.* **2002**, *83*, 3470.
- (16) Brown, M. S.; Goldstein, J. L. *Science* **1976**, *191*, 150.
- (17) Vitols, S.; Peterson, C.; Larsson, O.; Holm, P.; Aberg, B. *Cancer Res.* **1992**, *52*, 6244.
- (18) Hevonoja, T.; Pentikainen, M. O.; Hyvonen, M. T.; Kovanen, P. T.; Ala-Korpela, M. *Biochim. Biophys. Acta* **2000**, *1488*, 189.
- (19) Kascakova, S.; Refregiers, M.; Jancura, D.; Sureau, F.; Maurizot, J. C.; Miskovsky, P. *Photochem. Photobiol.* **2005**, *81*, 1395.
- (20) Gbur, P.; Dedic, R.; Chorvat, D., Jr.; Miskovsky, P.; Jancura, D. *Photochem. Photobiol.*, in press.
- (21) Mukherjee, P.; Adhikary, R.; Halder, M.; Petrich, J. W.; Miskovsky, P. *Photochem. Photobiol.* **2008**, *84*, 706.
- (22) Kascakova, S.; Nadova, Z.; Mateasik, A.; Mikes, J.; Huntuosova, V.; Refregiers, M.; Sureau, F.; Maurizot, J. C.; Miskovsky, P.; Jancura, D. *Photochem. Photobiol.* **2008**, *84*, 120.
- (23) Moskovits, M. *Rev. Mod. Phys.* **1985**, *57*, 783.
- (24) Aroca, R. *Surface-enhanced Vibrational Spectroscopy*; John Wiley & Sons: Chichester, 2006.
- (25) Wynn, J. L.; Cotton, T. M. *J. Phys. Chem.* **1995**, *99*, 4317.
- (26) Jancura, D.; Sanchez-Cortes, S.; Kocisova, E.; Tinti, A.; Miskovsky, P.; Bertoluzza, A. *Biospectroscopy* **1995**, *1*, 265.
- (27) Sanchez-Cortes, S.; Miskovsky, P.; Jancura, D.; Bertoluzza, A. *J. Phys. Chem.* **1996**, *100*, 1938.
- (28) Miskovsky, P.; Jancura, D.; Sanchez-Cortes, S.; Kocisova, E.; Chinsky, L. *J. Am. Chem. Soc.* **1998**, *120*, 6374.
- (29) Lajos, G.; Jancura, D.; Miskovsky, P.; Garcia-Ramos, J. V.; Sanchez-Cortes, S. *J. Phys. Chem. C* **2008**, *112*, 12974.
- (30) Lakowicz, J. R.; Geddes, C. D.; Gryczynski, I.; Malicka, J.; Gryczynski, Z.; Aslan, K.; Lukomska, J.; Matveeva, E.; Zhang, J.; Badugu, R.; Huang, J. *J. Fluoresc.* **2004**, *14*, 425.
- (31) Constantino, C. J. L.; Aroca, R. F. *J. Raman Spectrosc.* **2000**, *31*, 887.
- (32) Constantino, C. J. L.; Aroca, R. F.; Mendonc, C. R. S.; Mello, V.; Balogh, D. T.; Oliveira, O. N., Jr. *Spectrochim. Acta, Part A* **2001**, *57*, 281.
- (33) Maliwal, B. P.; Malicka, J.; Gryczynski, I.; Gryczynski, Z.; Lakowicz, J. R. *Biopolymers (Biospectroscopy)* **2003**, *70*, 585.
- (34) Cañameres, M. V.; Garcia-Ramos, J. V.; Sanchez-Cortes, S.; Castillejo, M.; Oujja, M. *J. Colloid Interface Sci.* **2008**, *326*, 103–109.
- (35) Lin, S.; Quaroni, L.; White, W. S.; Cotton, T.; Chumanov, G. *Biopolymers (Biospectroscopy)* **2000**, *57*, 249.
- (36) Romanchik, J. E.; Morel, D. W.; Harrison, E. H. *J. Nutr.* **1995**, *125*, 2610.
- (37) Verma, S. P.; Philippot, J. R.; Bonnet, B.; Sainte-Marie, J.; Moschetto, Y.; Wallach, D. F. H. *Lipids* **1985**, *20*, 890.
- (38) Schlucker, S.; Szeghalmi, A.; Schmitt, M.; Popp, J.; Kiefer, W. *J. Raman Spectrosc.* **2003**, *34*, 413.
- (39) Wang, P.; Nakamura, R.; Kanematsu, Y.; Koyama, Y.; Nagae, H.; Nishio, T.; Hashimoto, H.; Zhang, J. P. *Chem. Phys. Lett.* **2005**, *410*, 108.
- (40) Hoffmannova, H.; Hof, M.; Krtil, P. *J. Electroanal. Chem.* **2006**, *558*, 296.
- (41) Xu, S.; Szymanski, G.; Lipowski, J. *J. Am. Chem. Soc.* **2004**, *126*, 12276.

JP8112528